PHYSICAL REVIEW C VOLUME 22, NUMBER 2 AUGUST 1980

Limits on model-independent descriptions of elastic alpha-particle scattering

P. L. Roberson*
Department of Physics and Astronomy, University of Maryland, College Park, Maryland 20742
(Received 9 August 1979)

Nearly unconstrained parametrizations of local optical-model potentials are used to investigate potential shapes which best reflect experimental data. The model dependence of optical-model analyses is investigated by removing as much of the parametrization bias as is practical, so that the analyses are mostly dependent on the sensitivity of the alpha-nucleus interaction and the precision of the experimental data. It is found that real- versus imaginary-potential correlations are the dominant limitation on model-independent analyses using local potentials; correlations decrease the effective sensitivity of the interaction to the interior of the real potential and are responsible for ambiguous solutions to the problem.

[NUCLEAR REACTIONS α-nucleus optical potentials; model-independent parametrization. ^{50}Ti(α,α), E_α=140 MeV.]

I. INTRODUCTION

Relative nuclear-matter radii have been extracted from phenomenological optical-model analyses of elastic alpha-particle scattering for several isotopic sequences.[1,2] The results contain a bias and an inadequate error analysis because of the model dependence of the analysis procedures. In the absence of detailed knowledge of the alpha-nucleus interaction processes, we must consider both the real and imaginary potentials to be unknown, so that the use of any parametrization inserts a bias into the analysis of experimental data. The intention here is to minimize the bias by using nearly unconstrained parametrizations of local optical-model potentials to allow the estimation of realistic errors of extracted radii. Of primary interest are data sets which do not allow discrete ambiguities[3] in analyses using Woods-Saxon form factors because of their increased sensitivity to the radial shape of the potentials.[4]

The restriction of considering only local optical-model potentials represents a practical delimitation of the study. This restriction is in conflict with what is expected to be a realistic optical potential for alpha scattering at intermediate energies. The energy dependence of the real potential has been shown to be describable in terms of an energy-independent nonlocal potential.[5] In addition, contributions from reaction channels can be both large and nonlocal. For example, Wu *et al.*[6] measured the cross section for alpha-particle breakup to be greater than 30% of the total reaction cross section (independent of nucleus) for an incident alpha-particle energy of 160 MeV. The contribution to the optical potential from alpha-particle breakup is expected to be nonlocal, in analogy with the calculation of Johnson and Soper[7] for deuteron breakup. While a local potential may not provide a solution sufficiently close to nature to be useful for a detailed theoretical study of the alpha-nucleus interaction, this is not considered a dominant limitation on the extraction of *relative* mass-distribution information from such analyses.

To minimize the bias due to a particular choice of parametrization, the radial dependence of the potentials is chosen sufficiently unconstrained so that the analysis is dependent on the sensitivity of the scattering interaction and the precision of the experimental data. The sensitivity of the alpha-nucleus interaction is limited by the presence of both radial and real- versus imaginary-potential correlations. Radial correlations (in either the real or the imaginary potential) are the result of the nonlinear and nonlocalized relationship[8] between potential radius and scattering angle; real-versus imaginary-potential correlations are the result of the compensatory effects of varying the magnitude of the scattering and absorbing potentials simultaneously. The study of such correlations aids the understanding of the difficulties associated with obtaining a model-independent analysis of experimental data.

The analysis procedures are described in Sec. II. The results of computer calculations are given in Sec. III. Section IV contains the conclusions and suggestions for further study.

II. ANALYSIS PROCEDURES

Two calculational methods have been successfully used to remove constraints from the real potential: (1) Put and Paans[9] used cubic spline interpolation between radial points, whose magnitudes were chosen and then varied to obtain the best fit; (2) Friedman and Batty[10] added a Fourier-Bessel expansion to a (fixed) best-fit Woods-Saxon bias potential. Both spline and polynomial methods

place constraints on the potentials due to the practical limit to the number of radial points or polynomials which can be simultaneously varied. However, because their residual constraints are different, their comparison provides further information on the model dependence of the analysis.

An alternate approach is followed here. We generate a set of orthogonal polynomials capable of representing the optical potential in a manageable number of terms without the addition of a bias potential. The polynomials have the orthogonality requirement

$$\frac{1}{N_0}\int_0^\infty w(r)X_n(r)X_m(r)dr=\delta_{nm}\,, \tag{1}$$

where $w(r)$ is the weighting function (to be chosen), N_0 is the normalization constant, and

$$X_n(r)=\sum_{j=0}^{n}C_{nj}r^j \quad (C_{nn}\text{positive}) \tag{2}$$

are the polynomials. The normalization constant is determined by requiring $X_0=1$; the C_{nj} coefficients are calculated using the Gram-Schmidt orthogonalization procedure.[11] The choice of any weighting function continuous over the integration interval which allows the integral to exist will guarantee the existence of the polynomials. The set of polynomials are complete by Weierstrass's approximation theorem.[11]

The potential is

$$V(r)=w(r)\sum_{n=0}^{N}A_nX_n(r)\,. \tag{3}$$

All of the calculational convenience of working with orthogonal polynomials is preserved. The formulas are

(1) potential errors,

$$\Delta V(r)=w(r)\left((\chi^2/df)\sum_{n,\,m=0}^{N}X_n(r)X_m(r)\epsilon_{nm}\right)^{1/2}, \tag{4}$$

where χ^2/df is the χ^2 per degree of freedom and $\epsilon_{nm}=[\alpha^{-1}]_{nm}$ is the error matrix and where

$$\alpha_{nm}\cong\frac{1}{2}\frac{\partial\chi^2}{\partial A_n\partial A_m} \tag{5}$$

is calculated during the minimization procedure[12];

(2) volume integral of the potential,

$$J=4\pi\left(\int_0^\infty w(r)dr\right)\sum_{i=0}^{2}A_iB_i^0\,,$$
$$\Delta J=4\pi\left(\int_0^\infty w(r)dr\right)\left(\chi^2/df\sum_{i,j=0}^{2}B_i^0B_j^0\epsilon_{ij}\right)^{1/2}, \tag{6}$$

where the B coefficients are defined by the relation

$$r^{q+2}=\sum_{i=0}^{q+2}B_i^qX_i(r)\,; \tag{7}$$

and (3) moments of the radial function (odd moments are nonzero),

$$\langle r^q\rangle=\left(\sum_{i=0}^{q+2}A_iB_i^q\right)\Big/\left(\sum_{i=0}^{2}A_iB_i^0\right),$$
$$\Delta\langle r^q\rangle=\left(\chi^2/df\sum_{i,j=0}^{q+2}\frac{\partial\langle r^q\rangle}{\partial A_i}\frac{\partial\langle r^q\rangle}{\partial A_j}\epsilon_{ij}\right)^{1/2}, \tag{8}$$

where

$$\frac{\partial r^q}{\partial A_i}=\begin{cases}(B_i^q-\langle r^q\rangle B_i^0)\Big/\sum_{j=0}^{2}A_jB_j^0 & \text{for } i\le 2\,,\\ B_i^q\Big/\sum_{j=0}^{2}A_jB_j^0 & \text{for } 3\le i\le q\,.\end{cases} \tag{9}$$

The χ^2/df is computed using the formulas

$$\chi^2=\sum_{i=1}^{D}\left(\frac{\sigma_i^M-\sigma_i^C}{\Delta\sigma_i^M}\right)^2,$$
$$df=D-P\,, \tag{10}$$

where D and P are the number of data points and varied parameters, respectively, and the $\sigma_i^{M,C}$ are the measured and calculated differential cross sections and $\Delta\sigma_i^M$ are the cross-section errors. The validity of the error analysis is dependent on a $\chi^2/df\cong 1$. In the present calculations, the numerical errors in the calculation of the volume integral and low radial moments are one part in 10^5.

The number of terms required is minimized by choosing weighting functions equal to the form factors of a best-fit potential. Woods-Saxon-type form factors are used for convenience; in this case the nuclear part of the optical potential is

$$U_N(r)=[f(r,r_R,a_R)]^p\sum_{n=0}^{N}A_n^RX_n^R(r)$$
$$+if(r,r_I,a_I)\sum_{m=0}^{M}A_m^IX_m^I(r)\,, \tag{11}$$

where

$$f(r,r_0,a_0)=\left[1+\exp\left(\frac{r-r_0A^{1/3}}{a_0}\right)\right]^{-1}, \tag{12}$$

$p=1$ for Woods-Saxon (WS) polynomials, and $p=2$ for Woods-Saxon-squared (WS^2) polynomials. The $A_n^{R,I}$ are the varied parameters. Different initial-value conditions are obtained by changing the weighting functions and the number of terms in the expansions and by selected variation of parameters. The χ^2 is used as an estimate of quality of fit. Calculations were carried out using a modification of Perey's code **J1B3**.[13]

III. COMPUTER CALCULATIONS

Data for 140-MeV alpha-particle scattering from ^{50}Ti (Ref. 1) is used as an illustrative example.

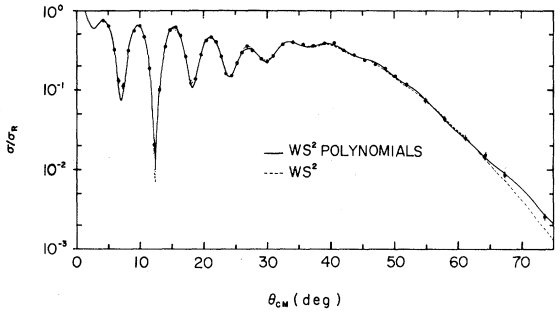

FIG. 1. Elastic scattering data for 140-MeV alpha particles from ^{50}Ti, plotted in ratio to Rutherford cross section versus center-of-mass angle. The curves are generated by the potentials shown in Fig. 2(a).

Figure 1 contains the data plotted in ratio to Rutherford scattering versus center-of-mass angle. The curves shown in Fig. 1 are generated by the best-fit potentials shown in Fig. 2(a): a WS^2-polynomial potential (with errors) and the WS^2 potential from Ref. 1 (shown only where it deviates from the polynomial curves in both figures). Small changes in both the real and imaginary potentials correct for the greatest discrepancies between the data and the WS^2-generated cross sections. The changes are predominantly potential shape variations not possible using WS or WS^2 parametrizations.

The radial dependences of the potential errors are in approximate agreement with radial sensitivity [Fig. 2(b)]. Figure 2(b) was generated using a notch test,[14] i.e., plotting the factor increase in χ^2 caused by a Gaussian perturbation as a function of radius for the real and imaginary potentials separately. Radial errors are underestimated at the very small and very large radii where the sensitivity curve is essentially unity. The range of validity for the potential plus errors is 1 to 9 fm (real potential) and 3 to 8 fm (imaginary potential).

The study of parameter correlations is facilitated by plotting the difference between computer-generated curves and the experimental data. Differences between the computed cross section of the polynomial fit and the data or WS^2-generated cross sections are given in Fig. 3(a). The same curves for the notch test are plotted in Fig. 3(b). There is an extended region of the real potential which has a significant effect on the large-angle behavior; this illustrates radial correlations within a potential part. Correlated changes between the real and imaginary potentials can keep the behavior of the cross section essentially unchanged. Both of these correlations increase errors beyond what would be expected from the notch test.

Correlations also cause multiple solutions of comparable quality. Potential curves and parameters of two independent solutions are given in Fig. 4 and Table I, respectively. The predominant difference is a shift in both real and imaginary potential strengths in the 4–6 fm region, demonstrating the effect of the real-imaginary potential correlations. The two solutions are independent in the sense that there is no straightforward extrapolation between the minima in χ^2 space. They are presented using the polynomials generated from the

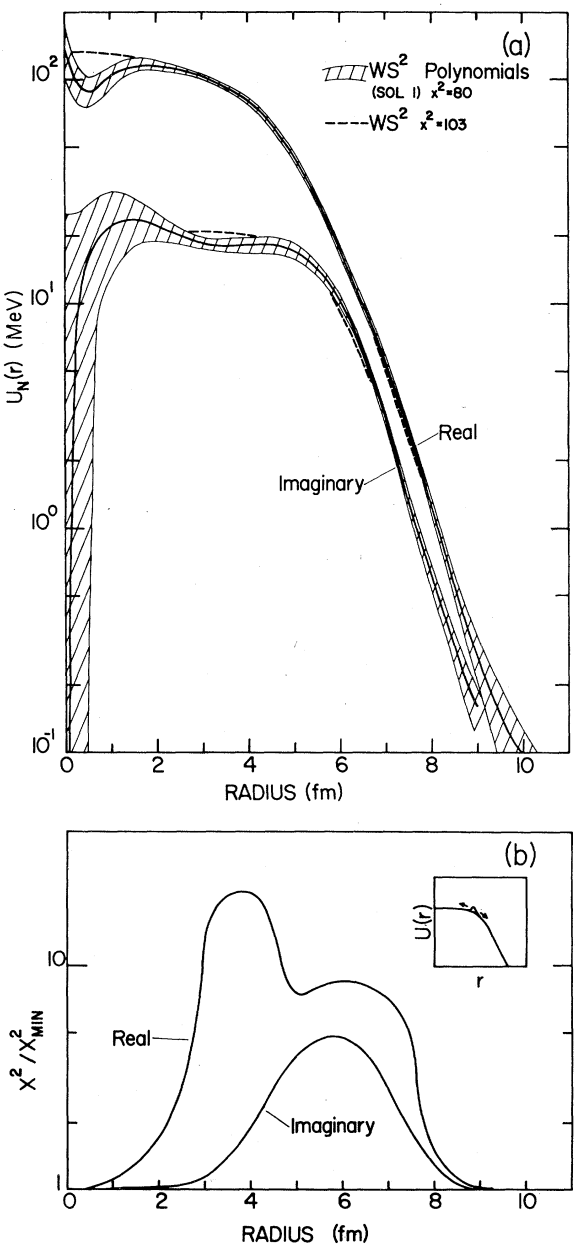

FIG. 2. (a) Comparison of a WS^2 polynomial fit to the best-fit WS^2 potential of Ref. 1. (b) Sensitivity curves generated by adding a notch perturbation (as sketched in the inset) to the real and imaginary potential separately.

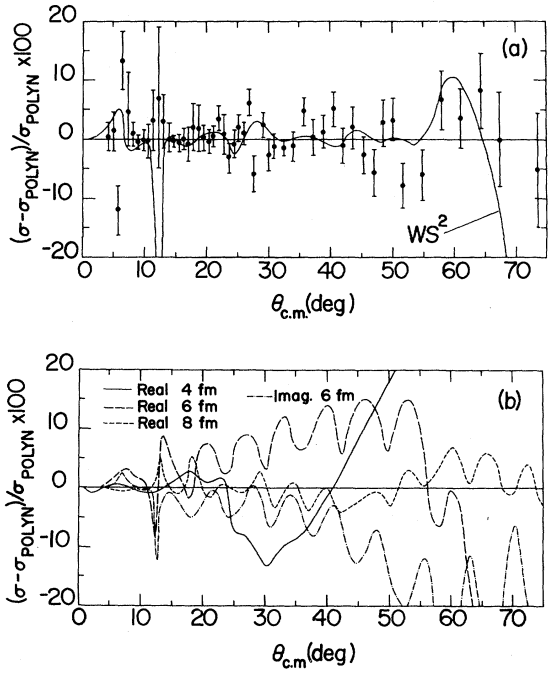

FIG. 3. Percent change in the center-of-mass cross sections with respect to those generated by the WS²-polynomial potential shown in Fig. 2(a). (a) Comparison with the experimental data and with the cross sections generated by the WS² potential (Ref. 1); (b) effect on the cross sections of the notch perturbation for the potential part and radius indicated.

best-fit WS² potential of Ref. 1 in order to easily compare potential properties of both polynomial and WS² potentials. A minor shift in weighting-function values for the imaginary potential reduce the χ^2 values to 60 for "solution 1" and 52 for "solution 2." Obviously, the χ^2 minimum is too strong a function of the type of parametrization chosen to rigorously apply statistical methods to choose among the various solutions.

Optimally unbiased results are obtained by comparing results of various potential parametrizations. We investigated the two solutions with the spline technique, which is not as constrained to smooth variations over extended radial regions. In Fig. 5, a spline solution is compared to the two polynomial fits already presented. This solution depends on the choice of radial points, but is still representative of the ambiguities resulting from correlations. Tests of the independence of the spline potentials investigated showed that (1) the spline counterpart of the polynomial solution-1 potential is independent of the spline solution shown in Fig. 5, and (2) the spline curve of Fig. 5 can be made to look similar to the polynomial solution-2 potential, but at a χ^2 of 73 compared to 61 (spline minimum) and 55 (solution-2 minimum). Because different parametrizations are not expected to have identical best-fit χ^2's for similar potentials, only two independent solutions have been found.

TABLE I. Comparison of potential parameters for fits to alpha-particle scattering from ^{50}Ti. Weighting-function values are $r_R = 1.4363$, $a_R = 1.1825$, $p = 2$, $r_I = 1.5884$, and $a_I = 0.6253$.

Parameters (in MeV)	WS² polynomial solution 1	WS² polynomials solution 2	WS²
A_0^R	125.1 ±4.8	117.9 ±1.6	136.0
A_1^R	13.5 ±5.1	14.5 ±3.1	
A_2^R	−4.5 ±4.7	−12.3 ±2.5	
A_3^R	3.5 ±5.3	4.7 ±3.6	
A_4^R	11.2 ±8.1	−1.4 ±8.7	
A_5^R	15.5 ±16	−9.8 ±16	
A_6^R	33.7 ±22	−8.3 ±27	
A_7^R	38.9 ±28	−19.5 ±33	
A_8^R	45.2 ±24	−25.8 ±31	
A_9^R	28.5 ±15	−17.2 ±19	
A_{10}^R	15.9 ±6.2	−11.3 ±7.6	
A_0^I	19.7 ±3.4	14.8 ±1.6	20.9
A_1^I	1.6 ±3.9	5.2 ±1.8	
A_2^I	−1.3 ±3.2	−2.1 ±1.4	
A_3^I	1.7 ±3.3	4.3 ±2.4	
A_4^I	−2.4 ±2.6	2.7 ±2.1	
A_5^I	1.4 ±3.4	5.3 ±4.1	
A_6^I	−2.0 ±2.5	4.1 ±2.9	
A_7^I	−0.5 ±2.1	1.8 ±2.7	
$J^R/4A$ (MeV fm³)	306.6 ±5.9	286.8 ±8.6	301.2
$\langle r \rangle_R$ (fm)	4.33±0.05	4.23±0.06	4.242
$\langle r^2 \rangle_R$ (fm)	4.63±0.07	4.48±0.09	4.513
$\langle r^3 \rangle_R$ (fm)	4.93±0.12	4.70±0.16	4.754
$J^I/4A$	97.5 ±4.0	89.6 ±2.5	97.6
$\langle r \rangle_I$ (fm)	4.90±0.07	5.16±0.09	4.855
$\langle r^2 \rangle_I$ (fm)	5.13±0.09	5.48±0.14	5.092
σ_R (mb)	1562	1687	1555
χ^2/df	2.4	1.7	2.2

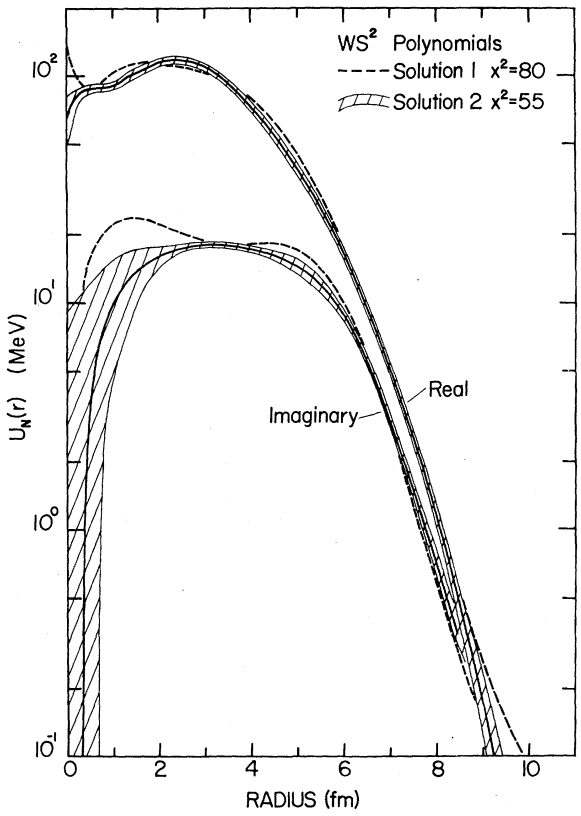

FIG. 4. Comparison of a second WS^2-polynomial potential to the polynomial potential shown in Fig. 2(a).

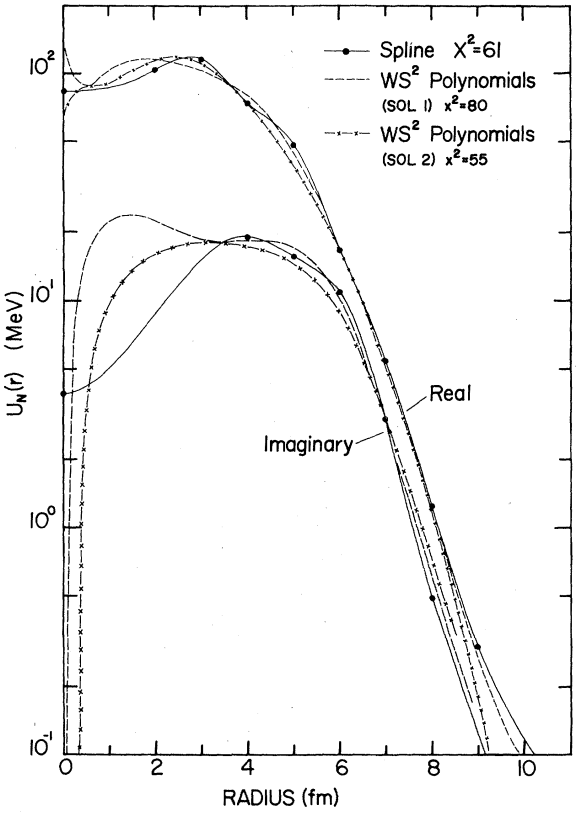

FIG. 5. Comparison of a best-fit spline potential to the WS^2-polynomial potentials.

The acceptable fits give a great variety of solutions even within one type of solution. The variations in the real potential for many acceptable solutions are shown in Fig. 6. The variations found for the three solution-1 potentials make it difficult to accurately quote a single potential with errors. However, the best-fit spline, WS polynomial, and WS^2 polynomial soultion-1 potentials (χ^2 between 59 and 70) have variations in the volume integrals and radial moments in good agreement with the quoted errors of Table I. Unfortunately, the solution-1/solution-2 ambiguity makes any statement of potential errors highly suspect. Similar ambiguities exist in the analyses of the ^{46}Ti and ^{48}Ti (Ref. 1) data as well.

The absolute values of the χ^2 and χ^2/df should be interpreted carefully. The derivation of the χ^2 function assumes uncorrelated errors, which is not the case. For example, correlated errors based on the uncertainty in the scattering angle contributes a 15% uncertainty in the χ^2 for the ^{50}Ti data. In addition, the true number of degrees of freedom is in doubt because of correlations between both data point errors and model parameters. Nevertheless, the statistical probability of obtaining a χ^2/df of 1.7 ± 0.3 for 33 ± 5 degrees of freedom (the ^{50}Ti best case) is less than 10%. This indicates that the present parametrizations are statistically inadequate to represent the data, which is not surprising because of the restriction to the use of local potentials only.

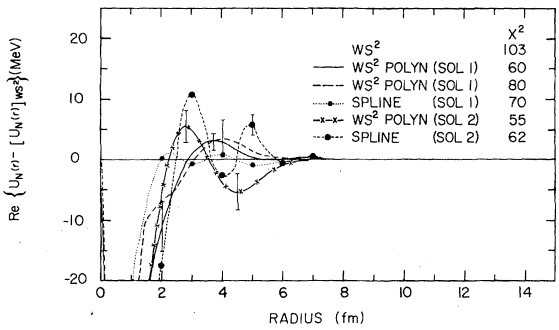

FIG. 6. The difference between the real part of several polynomial and spline potentials and the WS^2 potential of Ref. 1. The sol. 1 or sol. 2 labeling represents their approximate classification as described in the text. Potentials shown earlier can be identified by a comparison of χ^2 values.

IV. CONCLUSIONS

We have shown that nearly unconstrained parametrizations of local optical-model potentials allow potential correlations to dominate the analysis of the experimental data. These correlations make it difficult to locate a well-defined χ^2 minimum. The closest we can come to a model-independent description is to state the properties of a collection of similar best-fit potentials for each independent solution found. The unbiased estimate of the error on the rms radius (*for any one solution*) of the real potential, obtained by combining the average "statistical" errors [given by Eq. (8)] with the spread of the mean values for the best-fit potentials, is approximately 0.1 fm. However, the presence of *additional*, independent solutions makes the statement of a simple model-independent error impossible. Therefore, the extraction of rms radii from these types of potentials is probably not useful for determinations of relative rms radii of the mass distributions without additional isotopically unvarying assumptions. This is dramatically illustrated in Fig. 6: Including all possible best-fit potentials in the analysis allows very little information to be obtained.

We have also shown that the dominant mechanism allowing the existence of the many solutions shown in Fig. 6 is the real- versus imaginary-potential correlations. Thus, the true range of possible potentials cannot be determined if an overly constrained imaginary-potential parametrization is used. In addition, a reasonable χ^2 fit to the data does not necessarily guarantee that useful mass-distribution information can be obtained from the potential. If it is possible to determine the dominant mechanism for the isotopic (or other) dependence of the imaginary potentials, then an isotopically unvarying contribution to the imaginary potential could be used. The effect on relative radii of such an (unconstrained) contribution may be small. This would be a weaker model-dependent assumption than is currently used.

Freindl *et al.*[15] have investigated the energy dependence of real- versus imaginary-potential correlations, and have found that the resulting ambiquities are much greater for lower incident energies [$E_\alpha = 40$ and 59.1 MeV compared to $E_\alpha = 99.5$ and 118 MeV for $^{90}\mathrm{Zr}(\alpha,\alpha)^{90}\mathrm{Zr}$]. The low-energy data were fitted by using low-constraint parametrizations for *either* the real potential *or* the imaginary potential. This contrasts with the higher-energy data where (as shown here) *both* the real and imaginary potential must have low-constraint parametrizations to demonstrate a substantial ambiguity. Therefore, the probability of an incorrect imaginary potential causing an artificial bias of real-potential properties is increased for analyses of low-energy data.

Model-dependent folding parametrizations may provide information on relative mass distributions in spite of the strong correlations present in the problem. In the 6–8 fm region, where the real potential is unambiguously determined by the diffraction scattering, effects due to an unknown imaginary potential may be sufficiently small to allow relative mass distributions to be determined. The model-dependent errors could be estimated.

The contribution to the errors due to potential correlations can be reduced by a better determination of the scattering cross sections at the larger angles, particularly greater than ~50° for the ^{50}Ti case. This would provide a more stringent test for the phenomenological potentials, but may not improve the reliability of the extraction of information on relative mass distributions.

ACKNOWLEDGMENTS

The author thanks Dr. D. A. Goldberg, Dr. E. F. Redish, and Dr. N. S. Wall for many stimulating discussions. The computer calculations were made possible by a grant from the University of Maryland Computer Science Center. This work was supported in part by the National Science Foundation.

*Present address: National Cancer Institute, NIH, Bethesda, Md. 20205.

[1]P. L. Roberson, D. A. Goldberg, N. S. Wall, L. W. Woo, and H. L. Chen, Phys. Rev. Lett. 42, 54 (1979).

[2]See, for example, H. Rebel, H. J. Gils, E. Friedman, and Z. Majka, in Proceedings of the 2nd Louvain-Cracaw Seminar, edited by G. Gregoire and K. Grotowski (unpublished), p. 393; A. Budzanowski, C. Alderliesten, J. Bojowald, W. Oelert, P. Turek, H. Dabrowski, and S. Wiktor, contribution to the International Discussion Meeting, Karlsruhe, 1979 (unpublished).

[3]D. A. Goldberg and S. M. Smith, Phys. Rev. Lett. 29, 500 (1972).

[4]D. A. Goldberg, Phys. Lett. 55B, 59 (1975); A. A. Cowley and N. S. Wall, Phys. Rev. C 17, 1322 (1978).

[5]D. F. Jackson and R. C. Johnson, Phys. Lett. 49B, 249 (1974).

[6]J. R. Wu, C. C. Chang, H. D. Holmgren, and R. W. Koontz, Phys. Rev. C 20, 1284 (1979).

[7]R. C. Johnson and P. J. R. Soper, Phys. Rev. C 1, 976 (1970).

[8]Even classically, the particle trajectory samples a range of potential radii. Quantum mechanically, the trajectories are blurred by the de Broglie wavelength

of the particle and are mutually interfering.
[9]L. W. Put and A. M. J. Paans, Nucl. Phys. A291, 93 (1977). In addition, A. M. Kobos and R. S. Mackintosh have used the spline technique on both real and imaginary potentials to analyze proton scattering data (unpublished).
[10]E. Friedman and C. J. Batty, Phys. Rev. C 17, 34 (1978).
[11]See R. Courant and D. Hilbert, *Methods of Mathematical Physics* (Interscience, New York, 1953).
[12]See P. R. Bevington, *Data Reduction and Error Analysis for the Physical Sciences* (McGraw-Hill, New York, 1969). Note that the formula for parameter correlations given in Ref. 10 is in disagreement with Bevington: $\langle \Delta A_n \Delta A_m \rangle$ (Ref. 10) = $(df/2)\langle \Delta A_n \Delta A_m \rangle$ (Bevington).
[13]F. G. Perey, private communication.
[14]J. G. Cramer, University of Washington progress report, 1976 (unpublished); N. S. Wall, A. A. Cowley, R. C. Johnson, and A. M. Kobos, Phys. Rev. C 17, 1315 (1978).
[15]L. Freindl, H. Dabrowski, K. Grotowski, and R. Planeta, Institute of Nuclear Physics, Cracow, Report No. 1059/PL (unpublished).